DYNAMICS OF THE GAS IN SPIRAL GALAXIES

William W. Roberts, Jr.

University of Virginia
Charlottesville, Virginia

ABSTRACT

The dynamics of the gaseous component in disk-shaped galaxies is
thought to play an important governing role in star formation, mole-
cule formation, and the degree of development of spiral structure. The
prospect that density waves and galactic shock waves are present on the
large-scale has received support in recent years from a variety of ob-
servational studies. Large-scale shocks provide a most promising
mechanism for driving star-forming and molecule-forming events on the
scales of many kpc along spiral arms. Such shocks may also govern the
kinematics and relative distribution of various galactic tracers. This
is particularly apparent in M81 and other external spirals, because of
our "bird's-eye-view" perspective, and for the tracers of HI and CO in
our own Galaxy. Comparison of the CO observations with model simula-
tions based on the precepts of the density wave theory shows that these
precepts are supported by several observational results.

INTRODUCTION

In this review we focus on the large-scale distribution and dyna-
mics of the gas in spiral galaxies. It was observations of external
spirals which for the most part motivated the density-wave interpreta-
tion of spiral structure. According to this interpretation, which orig-
inated with Lindblad (1963) and which has been developed toward a coher-
ent theory by Lin and his colleagues and others(see Lin 1971), many ob-
served characteristics of a spiral arm are attributed to the recent
passage through the interstellar medium of the crest of a spiral density
wave.

GALACTIC SHOCK WAVES

In such a passage a large-scale galactic shock wave can develop in

W.W. Roberts, Jr.

the ambient interstellar medium (Roberts, 1969; Roberts and Yuan, 1970; also see Fujimoto, 1968). Figure 1 following Roberts and Yuan (1970, for the case of a one component gas e.g. "Phase I" gas clouds) illustrates the location of the shock formed along the background spiral arms (left panel). Undergoing rapid basic rotation about the galactic center, the gas flows along the arrowed streamlines through the slower rotating wave pattern from one shock to the next. It is mainly the spiral gravitational field of the background pattern coupled with rotation along with the effect of pressure and the variation in streamtube cross section that drives the gaseous response and forms the shock. The galactic magnetic field and the cosmic ray particles which interact with the magnetic field also constrain the gas motion. In the model here, a galactic magnetic field is embedded in the gas, and the shock that forms is a hydromagnetic shock wave. Because of the enormous size of the galaxy, the magnetic field is essentially "frozen into" the gas, and the arrowed streamlines represent the gas streamlines as well as the magnetic lines of force.

Galactic shock waves may well form a possible triggering mechanism for the gravitational collapse of gas clouds, leading to star formation and the formation of other tracers along spiral arms. Figure 2 from Roberts (1969) provides a sketch of the nonlinear response of the gas density distribution along a streamline and illustrates this possible star formation mechanism. Gas flows into the shock and compression region from left to right. Before reaching the shock, some of the large clouds and cloud complexes may be on the verge of gravitational collapse. A sudden compression of the clouds in the shock could conceivably trigger the gravitational collapse of some of the largest gas clouds. As the gas leaves the shock region, it is rather quickly decompressed, and star formation ceases.

WARM, NEARLY NEUTRAL, INTERCLOUD "PHASE II" GAS

Shu et. al. (1972) show that the shock phenomenon can work rather efficiently in the two-phase picture of the interstellar medium put forward by Pikelner (1967), Field Goldsmith and Habing (1969), and Spitzer and Scott (1969), which pictures the nearly neutral component of the interstellar medium to consist of two gaseous phases in rough pressure equilibrium with one another: cold, dense "Phase I" clouds at temperatures of 20-200°K embedded in a warm rarefied "Phase II" intercloud medium at temperatures of 10^3-10^4°K. The existence of such a neutral, warm, rarefied intercloud medium is suggested by the fact that emission line profiles show broad wings which are absent in the absorption lines found in the directions toward discrete radio continuum sources (Clark 1965; Hughes, Thompson, and Colvin, 1971; Radhakrishnan et. al., 1972; and Shu, 1977; however also see Steigman, Strittmatter, and Williams, 1975). In this picture, the clouds are viewed as embedded bodies which expand or contract to adjust to changes of the ambient pressure of the intercloud medium; and the increase in pressure across
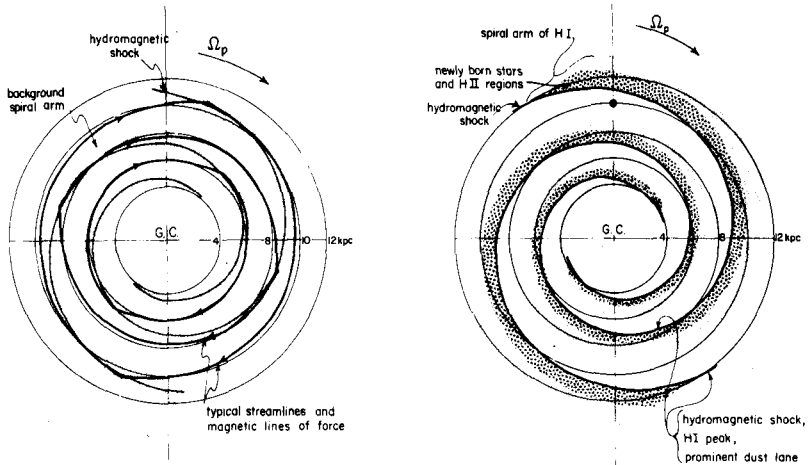
Figure 1. (Left panel) Schematic of a background spiral density wave pattern and the nonlinear gas response. Shocks form along the background spiral arms. Each gas streamline appears as a sharp-pointed oval with a sharp turning point at each shock. (Right panel) Schematic of the internal structure and temporal sequence expected across a spiral arm delineated by a large-scale shock (from Roberts 1969 following Roberts and Yuan 1970).
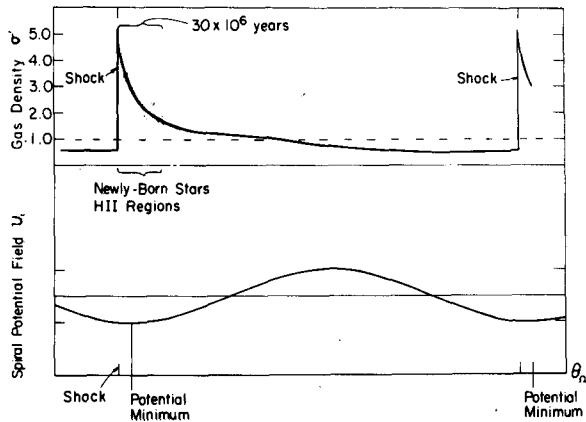

Figure 2. Distribution of gas density, relative to the underlying (stellar) gravitational potential, along a typical streamline (from Roberts 1969). The regions of strong compression, in which molecule and star formation may be prominent, lie within and just outside the shock. The shaded area shows the extent of these objects corresponding to a formation and evolution time of 30 million years.

the galactic shock occurring in the "warm" intercloud phase is in turn
transmitted to the "cold" clouds, leading to star formation. Woodward
(1976) carries out quantitative studies of the shock-driven implosion
of cold clouds embedded in compressed intercloud material, and his re-
sults suggest in considerable detail how star formation can proceed on
the small scale.

SPIRAL SHOCKS WITHOUT SPIRAL FORCING

     The formation of such large amplitude spiral waves in the gas is
not greatly sensitive to the form of the background forcing field
adopted to drive the gas. For example, in time-dependent, two-
dimensional, numerical, hydrodynamical studies of the gas response to
bar-like oval distortions and prolate spheroidal perturbations, Sanders
and Huntley (1976) and Huntley, Sanders, and Roberts (1977; also see
Sorensen, Matsuda, and Fujimoto, 1976) find large amplitude wave
patterns of rather similar character, but with rather open spiral arms.
Figure 3 from Huntley et. al. (1977) shows a photographic simulation of
the gas density distribution in response to a mild bar-like forcing, for
one of the cases considered.

Figure 3. Photographic simulation of the gas density distribution in
response to a mild bar-like oval distortion (from Huntley, Sanders, and
Roberts 1977). The intensity scale is logarithmic, ranging from 0.1
H-atoms cm^{-2} (black) to 1.0 H-atoms cm^{-2} (white). Each photographic
square represents one cell of the (80 × 80) numerical grid. The major
axis of the perturbing potential is the horizontal axis.

TWO REGIMES OF GAS FLOW

Galactic shocks form if the driving force F of the interstellar gas, which may be contributed by the spiral gravitational field of the stars or by a bar or by other means, is sufficiently strong so as to force the velocity component normal to a spiral arm $W_\perp$, to oscillate at transonic speeds about its unperturbed value, $W_{\perp o}$ (7-12 km/s is the effective acoustic speed   a   for "Phase I" and "Phase II" gas). Figure 4 shows that there are actually two different regimes of shocked gas flow (Shu et. al., 1973, for a "Phase I" gas). For regime (1), with $W_{\perp o}$ > effective acoustic speed   a   (left panel), the shocks are strong and produce narrow zones of high gas compression (as in Figure 2). For regime (2), with $W_{\perp o}$ < effective acoustic speed (right panel), the shocks are weak or absent and yield broad zones of low compression. This difference may underlie the observed differentiation between the narrow, filamentary spiral arms, observed in some galaxies and the broad, massive spiral arms observed in others.
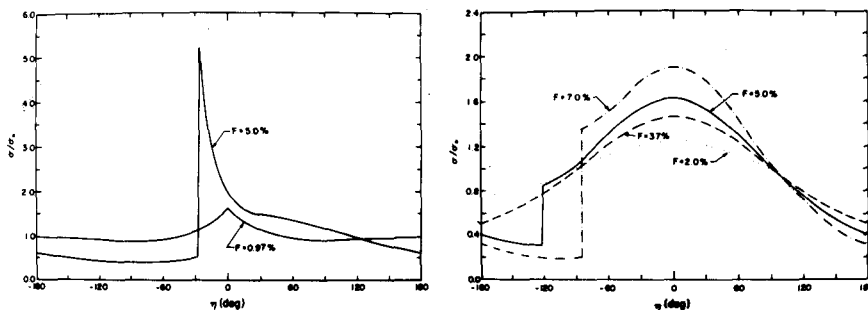

Figure 4. Variation of the density enhancement σ/σ_o as a function of phase η between adjacent arms, for various strengths F of the driving field, showing the distinction between the nonlinear and linear regimes (from Shu et al. 1973). Regime (1), with $W_{\perp o}$ > effective acoustic speed, is characterized by strong shocks and narrow regions of high gas compression (left panel). Regime (2), with $W_{\perp o}$ < effective acoustic speed, is characterized by weak shocks (or no shocks) and broad regions of weak gas compression (right panel). The morphological characteristics of a given galaxy would depend on which regime is predominant.

SPIRAL STRUCTURE IN EXTERNAL SPIRALS

Van den Bergh (1960a,b) shows that the intrinsic luminosity of a spiral galaxy is related to the qualitative appearance of the spiral arms. Galaxies with prominent, narrow spiral arms are intrinsically the most luminous, while galaxies exhibiting patchy broad arms have the lowest intrinsic brightness. If star-forming efficiency is related to the compression suffered by the gas, and if the width of the spiral arm

W.W. Roberts, Jr.

(as measured by the angular extent of recently-formed stars) is related
to the width of the region of high compression, then one expects those
galaxies characterized by large values of $W_{\perp o}$ to have the narrowest,
most prominent arms. Figure 5 from Roberts et. al. (1975) shows for
24 representative galaxies the relationship between $W_{\perp o}$ and potential
shock strength on the one hand, and luminosity classification and the
degree of development of spiral structure on the other. Those galaxies
with potentially strong shocks show well-developed spiral structure,
while those for which weak or no shocks are predicted via the $W_{\perp o}$
parameter show poorly-developed structure. Other parameters such as the
driving force F and the gas content are expected to play important
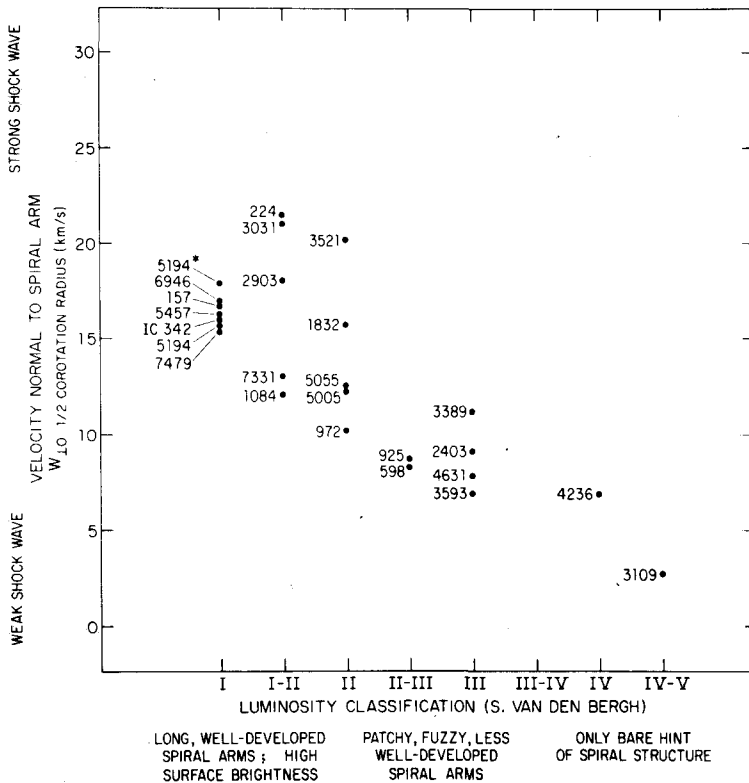roles as well.

Figure 5. Variation of the kinematic parameter $W_{\perp o}$ with luminosity
classification for 24 representative spirals (from Roberts et al 1975).
The correlation suggests that strong shocks are associated with well-
developed spiral structure; weak shocks are associated with poorly-
developed spiral structure.

M81 - A REPRESENTATIVE GALAXY

A representative galaxy characterized by regime (1) and large $W_{\perp o}$ is M81. Figure 6 shows an optical photograph of M81. The well-developed narrow spiral arms of the luminous star distribution are viewed to be a consequence of strong shocks. The observed surface density distribution of neutral hydrogen in M81, shown in Figure 7, also exhibits similarly well-developed spiral structure, extending to large distances from the center of the galaxy (Rots and Shane, 1975).
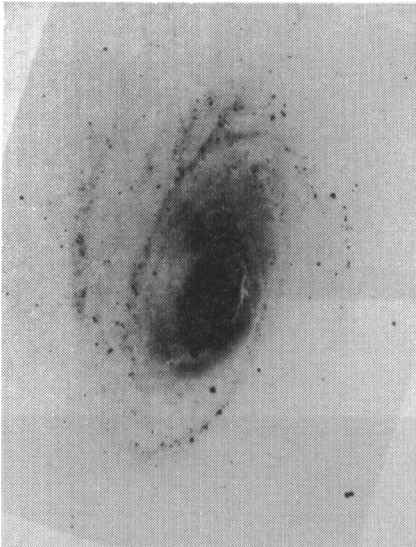

Figure 6. Negative, blue-light photograph of the sample galaxy M81, showing the well-developed narrow luminous spiral arms characteristic of strong galactic shocks (from Kitt Peak National Observatory).
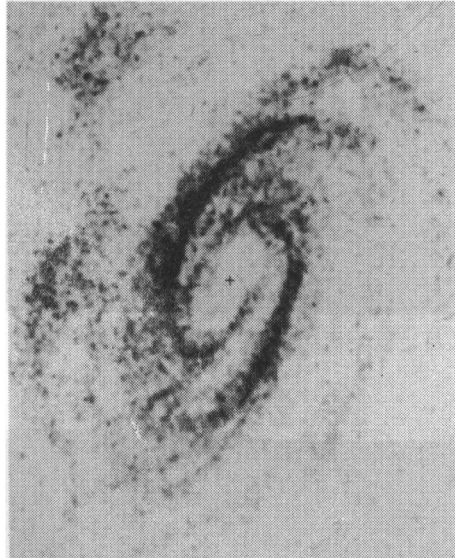
Figure 7. Radiograph of the HI surface density distribution in M81, showing that the gaseous arms are also narrow and well-defined (from Rots and Shane 1975). The scale of this figure is about half that of Figure 6.

Visser(1977) is able to focus in considerable detail on M81 by constructing a density wave model to simulate its dynamics. Figure 8 shows the locus of the potential minimum (----,dashed curve) of his theoretical two-armed spiral wave pattern superposed on an optical photograph of M81. The solid curve indicates the location of the shock which forms in the nonlinear gas flow in his model.

Figure 9 shows the unsmoothed velocity field for the gaseous component in Visser's model, superposed on the radiophotograph of the observed HI density distribution at 25" resolution from Rots and Shane

Figure 9. Map for M81 of the unsmoothed theoret- ical velocity field (symbols) for the gas cal- culated in the density wave model of Visser(1977) superposed on the radiograph of the observed neutral hydrogen surface density distribution (Rots and Shane 1975). The kink-like variations in the velocity contours locate the galactic shock along the observed spiral arms of neutral hydrogen (from Visser 1977).

Figure 8. Locus of the potential minimum (———, dashed line) of the background spiral arms in the density wave model for M81 of Visser (1977) super- posed on an optical photograph of M81. The solid line illustrates the location of the galactic shock wave which is formed in the nonlinear gas flow (from Visser 1977).
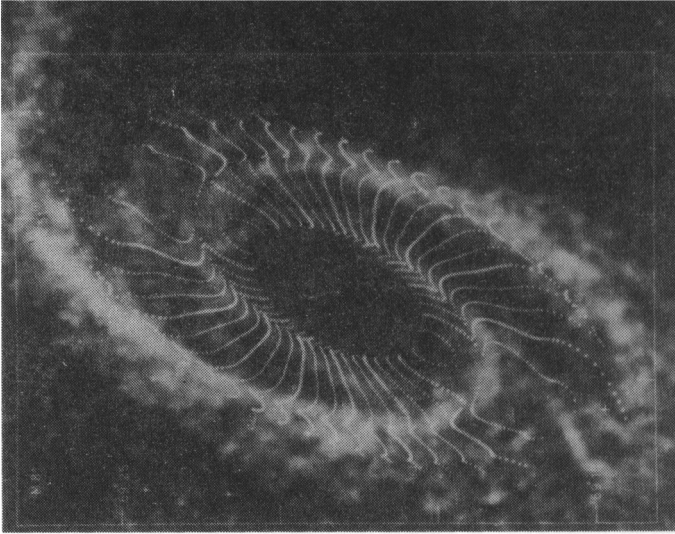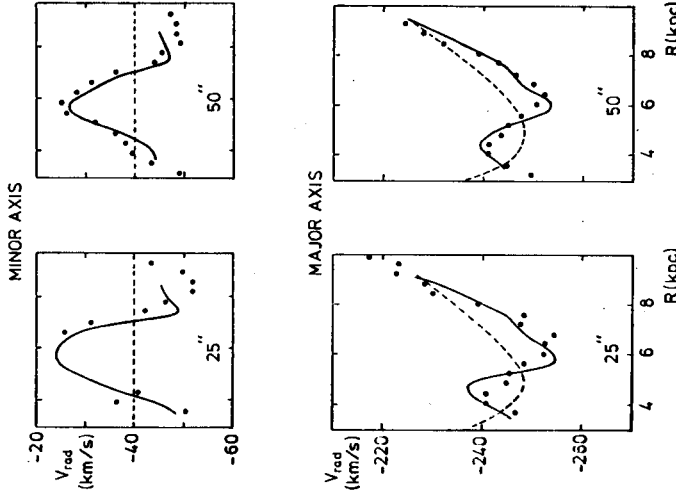
MINOR AXIS

MAJOR AXIS

Figure 11. Systematic motion of the gas in the density wave model (solid lines) for M81 of Visser (1977) along the minor and major axes smoothed to 25" and 50" resolutions, plotted in comparison with the observed systematic motion of the neutral hydrogen data at 25" and 50" resolutions (dots, Rots and Shane 1975). The dashed lines refer to an axisymmetric model of purely circular motion (from Visser 1977).
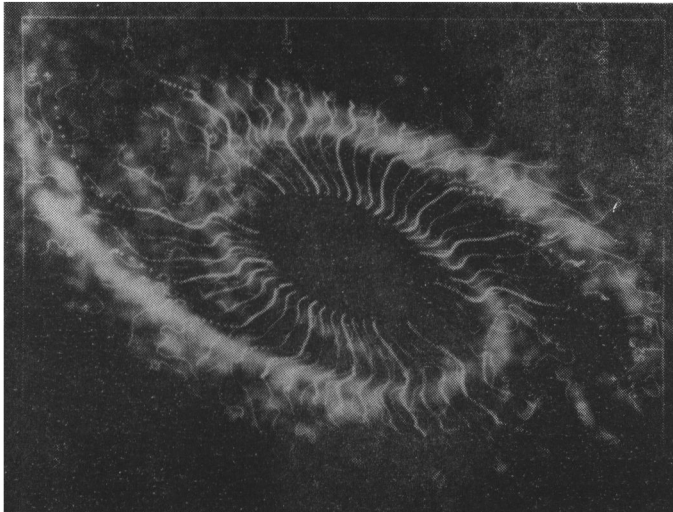

Figure 10 (from Visser 1977). Map for M81 of the (smoothed) theoretical velocity field for the gas (symbols) calculated in the density wave model of Visser (1977), smoothed to 25" resolution, plotted with the observed velocity field at 25" resolution (full and dashed lines, Rots and Shane 1975), superposed on the radiograph of the observed neutral hydrogen surface density distribution (Rots and Shane 1975).

W.W. Roberts, Jr.

(1975). The sequence of ordered kink-like variations in consecutive
velocity contours indicates the location of the shock where velocity
jumps from supersonic to subsonic are of the order of 30 km/s.

     In order to compare the theoretical density and velocity fields with
observations, Visser (1977) carries out an analysis to smooth the theo-
retical fields to the beam of the Westerbork radio telescope. Figure 10
shows the smoothed theoretical velocity field at 25" resolution (contours
of symbols) together with the observed velocity field at 25" resolution
(full and dashed lines), both superposed on the radiophotograph of the
observed HI density distribution at 25" resolution from Rots and Shane
(1975). The smoothed variations in consecutive velocity contours of the
model agree quite well with corresponding variations in the observed
velocity contours.

     Visser (1977) also smooths the theoretical velocity field to 50"
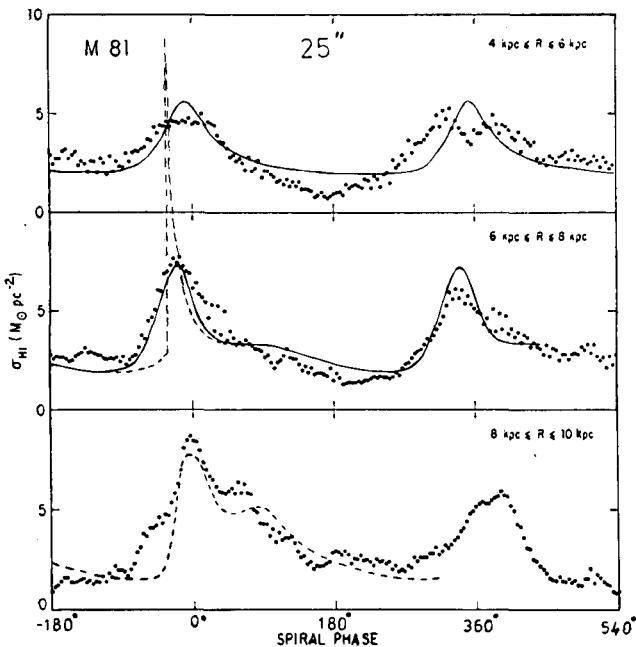and 2' resolutions and finds that the agreement with the observed veloc-

Figure 12 (from Visser 1977). Comparison of the observed HI surface
density distribution in M81 (dots, from Rots 1975) and the theoretical
gas density distribution in Visser's density wave model (solid lines),
both plotted with spiral phase within three annuli in the disk of M81.
The observed arm-interarm contrast and the skewed shape of the arm peaks
are rather well reproduced in the model.

ity field at these resolutions continues to be quite good. Figure 11
shows the velocity perturbations along the minor and major axes at 25"
and 50" resolution. The solid lines indicate the velocities of his
density wave model, the dashed lines indicate the velocities in an un-
perturbed axisymmetric model, and the dots illustrate the actual veloc-
ities of the observed data (from Rots and Shane 1975). A difference in
slopes at $\simeq 7$ kpc along the minor axis is apparent between the two reso-
lutions, in the correct sense expected in the theory.

Figure 12 (from Visser 1977) shows the observed HI surface density
distribution (dots) at 25" resolution from Rots (1975) plotted as a
function of spiral phase in three circular bands around M81, each 2 kpc
wide. The arm peaks of the observed data (dots) are substantially nar-
rower than the interarm troughs, altogether indicative of nonlinear wave
phenomena; and some peaks even show the skewed character of steep rise
and more gradual fall off, characteristic of strong shocks. Indeed the
solid lines represent the theoretical HI surface density distribution
in Visser's model (with shocks present), smoothed to 25" resolution,
and these show good agreement with the observational data (dots). The
sharp-peaked dashed line in the 6-8 kpc band illustrates an unsmoothed
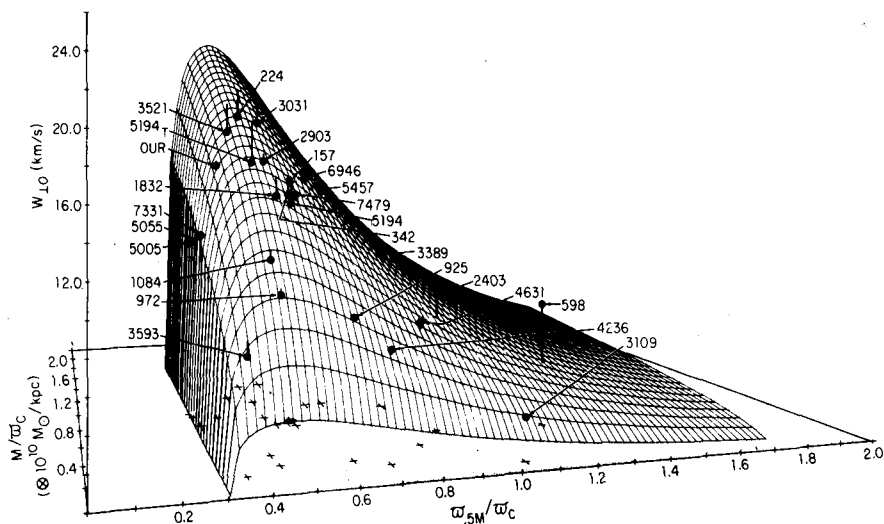shock profile.

Figure 13. Theoretical categorization of disk-shaped galaxies in the
two-dimensional parameter space of the fundamental quantities M/ϖ_c and
$\varpi_{.5M}/\varpi_c$ (from Roberts et al 1975). ϖ_c is the corotation radius and $\varpi_{.5M}$
is the radius inward of which lies half the total mass. Galaxies with
relatively large central concentration of mass (low $\varpi_{.5M}/\varpi_c$) e.g. M81 -
NGC 3031 are expected to have the strongest shocks.

OUR GALAXY IN THE PERSPECTIVE OF EXTERNAL SPIRALS

The parameter $W_{\perp o}$ and the shock strength in turn depend on two even more fundamental quantities: (1) the total mass of the galaxy divided by a characteristic dimension M/ϖ_c and (2) the degree of concentration of mass toward the galactic center, measured by $\varpi_{.5M}/\varpi_c$. Figure 13 from Roberts et al. (1975) shows this dependence. A galaxy as high on the $W_{\perp o}$ ridge as M81 (NGC 3031) can form strong shocks and thereby exhibit well-developed, narrow spiral arms. Our own Galaxy lies in the same general region of parameter space as M81, suggesting the possibility for similarly well-developed spiral structure.

We now turn to focus on our own Milky Way System. Hopefully these concepts of density wave theory which seem to play an important role in M81 and other external spirals, for which we enjoy a birds-eye-view perspective, can be borrowed and applied to help us better understand the structure and dynamics of our Galaxy.

RADIAL ABUNDANCE DISTRIBUTION OF INTERSTELLAR MATTER IN OUR GALAXY

Several observational aspects of the structure of our Galaxy are amenable to interpretation in the context of the density wave theory. One of the most impressive of such aspects concerns the different morphological characteristics of atomic hydrogen compared to those of all other constituents of the galactic disk which can be observed along transgalactic paths: the ionized and molecular states of hydrogen, CO and other molecules, supernova remnants, pulsars, γ-radiation, and synchrotron radiation. Figure 14 (from the review by Burton 1976) shows the radial distributions of several constituents of the galactic disk. With the exception of the HI, the overall shapes of these distributions are quite similar. On the other hand the diameter of the galactic disk as defined by atomic hydrogen is fully twice as large as that of the galactic disk as defined by these other constituents. Analogously for external galaxies, the HI disk is larger than the luminous disk (M. S. Roberts 1974). This separation of the peak concentrations of these tracers, representing recent and current activity, from that of the HI implies that there exists a factor other than the average HI density which controls the formation rate of molecules and stars. Furthermore, the rough equivalence of the inner Galaxy distributions suggests that a single mechanism is responsible.

Compression due to the passage of a galactic density wave and the associated shock has been invoked specifically to account for the relative HII regions/HI distributions (e.g., Mark 1971, 1974; Lin 1971; Shu 1973; Roberts 1975) and for the relative CO/HI and other distributions (Scoville and Solomon 1975, Burton et al. 1975, Gordon and Burton 1976). Figure 15 indicates schematically for our own Galaxy the regimes
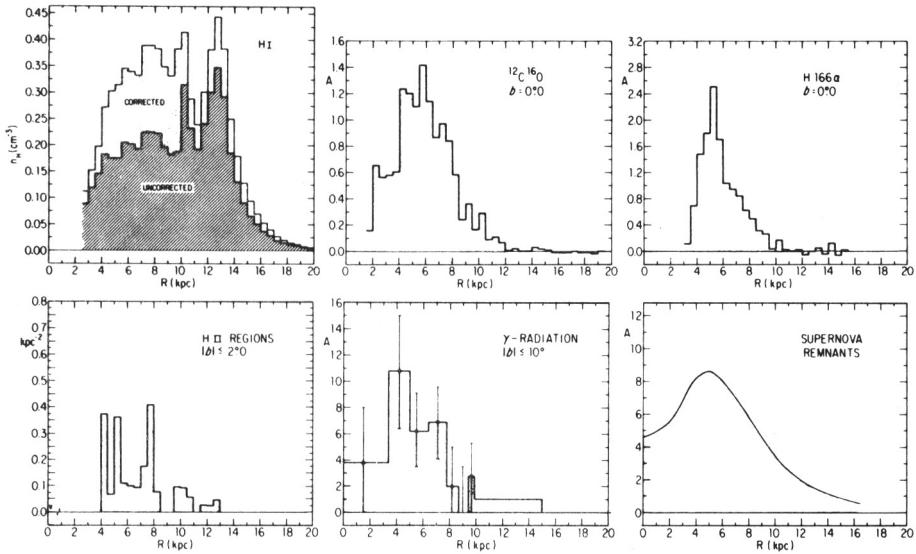
Figure 14. Radial abundance distributions of several constituents of
the galactic disk (from Burton 1976). The HI distribution is from
Burton (1976); the CO distribution is from Gordon and Burton (1976);
the H 166α distribution from Lockman (1976); that for giant HII
regions from Burton et al. (1975); the γ-ray distribution from
Strong (1975; see also Stecker et al., 1974); and that for supernova
remnants from Kodaira (1974). The abundance distributions for CO,
H 166α, HII regions, γ-radiation, and supernova remnants are substan-
tially more concentrated toward the galactic center than the abundance
distribution of HI.

of strong and of weak compression (Burton 1976, from the results of
Roberts et al. 1975). Strong shocks are possible in the inner Galaxy
because $W_{\perp o} >$ the effective acoustic speed. Here galactic shock fronts
may trigger molecular and stellar formation. In the outer region
compression is weak and conditions for molecular and stellar formation
are unfavorable except in unusual local environments. The inner Galaxy
is all the more susceptible to galactic shock influences because the
frequency at which the gas meets the spiral-wave pattern, $2[\Omega(\varpi)-\Omega_p]$,
increases with decreasing distance from the galactic center. Other as-
pects of the problem, including the dependence of compression efficiency
on ambient gas density, are dealt with by Oort (1973), Shu (1975), and
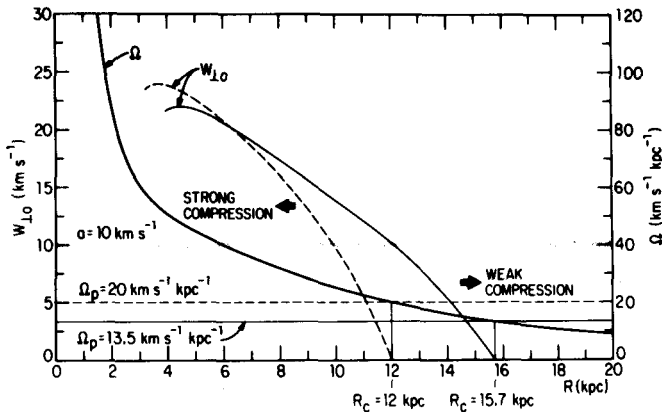Segalovitz (1975).

Figure 15. Schematic representation for our Galaxy of the variation of the density-wave parameter $W_{\perp o}$ calculated for two plausible values of the wave pattern speed, Ω_p. Relatively strong compression is expected in the inner Galaxy where $W_{\perp o} > a$, the effective acoustic speed in the interstellar medium. The frequency at which the shock wave acts on the gas, $2(\Omega - \Omega_p)$, also enhances the compression effects in the inner Galaxy.

CO AS A TRACER OF THE GALACTIC SHOCK IN OUR GALAXY

     The overall kinematics of CO are generally similar to those of HI (see Burton and Gordon 1977a,b). Figure 16 from Burton and Gordon (1977a) shows the CO terminal velocities plotted against longitude. The solid line represents the smooth rotation curve derived for our Galaxy. Ordered systematic variations of the CO terminal velocities from this line are apparent as crests near $\ell=52°$ and $\ell=32°$ and as a trough near $\ell=43°$. Similar systematic variations appear in the corresponding plot of HI terminal velocities (Burton and Gordon 1977a), with crests near $\ell=52°$ and $\ell=32°$, a trough near $\ell=43°$, and an additional trough near $\ell=24°$. These ordered variations can be readily understood in terms of streaming motions induced by the gravitational field of large-scale density perturbations in the overall galactic mass distribution. As such, they may represent direct observational evidence for spiral structure on the large-scale in our Galaxy (for the case of HI, see e.g., Yuan 1969, Burton and Shane 1970, Burton 1971). However, because these ordered variations, particularly in the CO data, are not more sharply confined in angle and of larger amplitude in velocity, it is natural to ask if the CO kinematics are consistent with the presence of large-scale shocks.

     Roberts and Burton (1977) address this question by following the dynamics of the cloud component in a spiral density-wave model with a
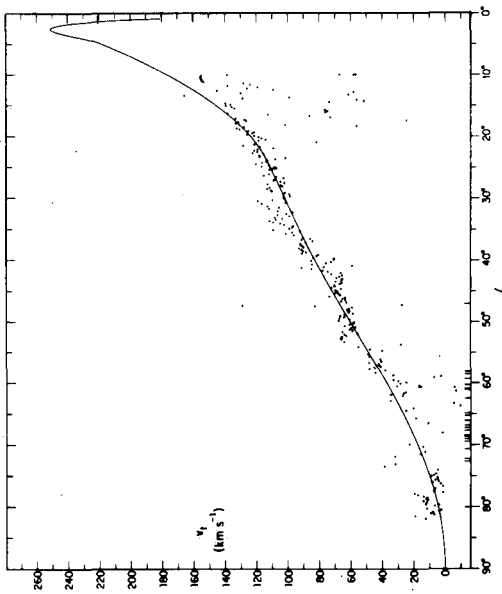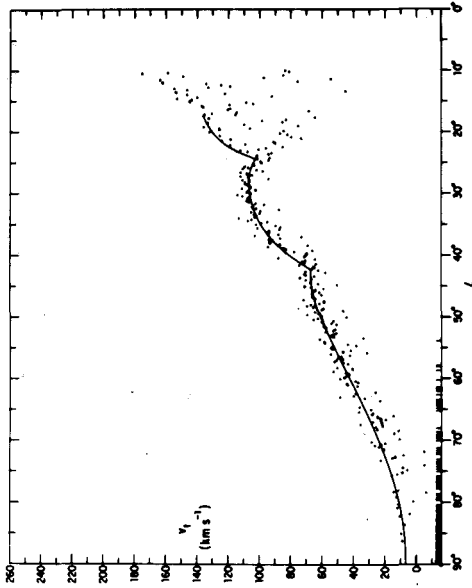
Figure 17. Distribution with longitude of the terminal velocities measured on the synthetic CO profiles (from Roberts and Burton 1977). The black line illustrates how the terminal-velocity locus predicted by the spiral model differs from that of the axisymmetric model for purely circular motion (grey line). The scatter in the points is due to the stochastic nature of the distribution. The ordered variations are due to the density-wave perturbation and reproduce the general trends observed.

Figure 16. Distribution with longitude of the terminal velocities measured on the observed CO profiles (from Burton and Gordon 1977a). The smooth black line illustrates the maximum line of sight velocity corresponding to the perturbation-free rotation curve for purely circular motion.

two-phase interstellar medium similar to that of Shu et al. (1972).
The cloud-intercloud medium interaction due to turbulent viscosity is
considered following Sawa (1975). The clouds themselves plow superson-
ically, as ballistic particles, through the shock and beyond until the
drag force due to turbulent viscosity slows them down (Bash and Peters
(1976) also consider ballistic cloud trajectories, but from a somewhat
different point of view). A smoothed peak forms in the overall density
distribution of the cloud component, in contrast to the sharply peaked
intercloud component.

     To compare the results of this spiral model with observations,
Roberts and Burton (1977) generate synthetic profiles at 0.2 intervals
of longitude, using the CO profile simulation method of Burton and
Gordon (1976, 1977a,b for an axisymmetric model). The spectra for the
spiral model are then processed by the same techniques and computer
programs used for the actual observations. Figure 17 shows the longi-
tude distribution of terminal velocities measured on the synthetic
profiles. The amplitude and locations of the ordered variations
resemble those observed (Burton and Gordon 1977a,b). The ordered
variations vary smoothly, despite the presence of large-scale shocks in
the model.

     Figure 18 shows side-by-side grey scale representations of the
velocity-longitude diagrams of the real CO observations (left, from
Burton and Gordon 1977a,b) and the synthetic CO emission of the spiral
model (right, from Roberts and Burton 1977). Both representations ex-
hibit similar clumpy arrangements of CO clouds. For the spiral model
(right) the large-scale feature lying between $\ell=10°$ and $\ell=35°$ and
the more extended feature at somewhat lower velocity extending up to
$\ell=60°$ correspond to spiral arms in the model. The clumpiness of these
large-scale spiral arm features is substantial despite the fact that
they originate from strong large-scale shocks. Both features can be
followed in the observed map (left), although they are even more patchy
and broken up over some regions. The additional degree of patchiness in
the observed map (left) may be due to the persistence of CO clouds over
longer time scales than those currently thought to be possible.

HOT, IONIZED, INTERCLOUD "PHASE III" GAS

     Recent satellite observations have now added a new dimension to
our perspective of the overall interstellar medium. The satellite
detection of OVI absorption and soft x-ray emission suggests that a
large fraction of the local intercloud medium near our sun may consist
of a hot, ionized, rarefied "Phase III" gas at temperatures of 2×10^5 -
10^6 °K (Jenkins and Meloy, 1974; Spitzer and Jenkins, 1975; Kraushaar,
1977). Mechanisms for producing such a medium have been considered by
Cox and Smith (1974), Castor, McCray, and Weaver (1975), Weaver et al.
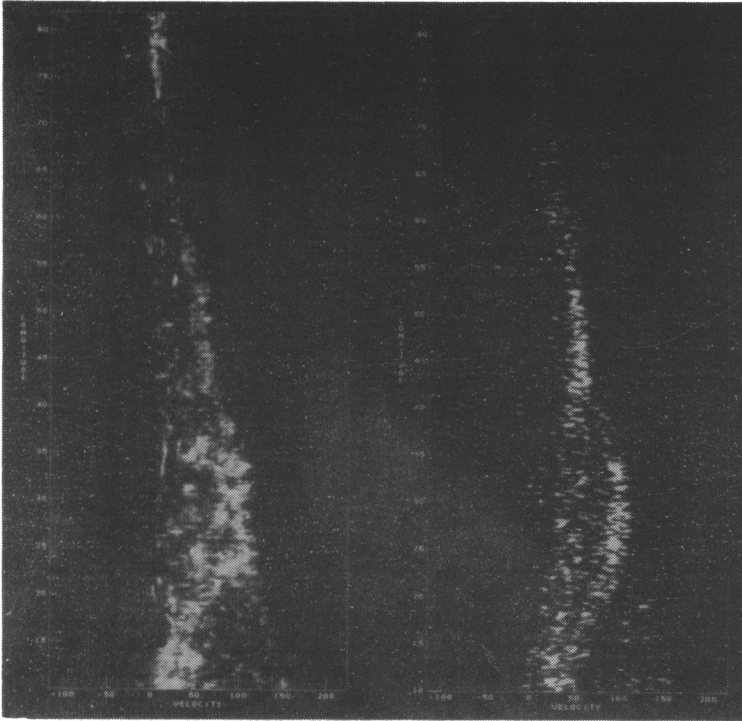(1977), and McKee and Ostriker (1977). Theoretical estimates of the

Figure 18.   (left) Grey-scale representation of the longitude, velocity arrangement of $^{12}C^{16}O$ emission observed at b = 0° (from Burton and Gordon 1977a,b). (right) Longitude, velocity arrangement of emission inherent in the synthetic line profiles, representing CO distributed stochastically in discrete clouds in the spiral model (from Roberts and Burton 1977). The clouds's kinematics and probability of occurrence follow the predict-ions of the density-wave theory.

filling fraction f of the "Phase III" gas based on the mechanism of overlapping supernova remnants vary over a wide range: f~0.5 (Cox and Smith 1974), f~0.3 (Smith 1977), and f~0.8 (McKee and Ostriker 1977). The diversity in these values for the filling fraction f signifies the considerable uncertainty involved in estimating the prevalence of "Phase III" gas (see Shu 1977).

    How extensive such "Phase III" gas is on the large-scale--beyond the local solar neighborhood--is very much an open question at the present time for another reason (Scott, Jensen, and Roberts 1977). If the large-scale intercloud medium in our Galaxy and external spirals were dominated by "Phase III" gas, as it seems to be in the solar neighbor-

hood, then the effective acoustic speed would be on the order of 100 km/s.
Consequently the formation of strong, large-scale shocks would be rather
difficult. A dynamically predominant "Phase III" medium on the large-
scale is therefore probably not characteristic of those spirals with
well-developed, filamentary spiral arms, or for the representative
galaxy M81 considered in detail herein, where galaxy-wide shocks provide
a most promising mechanism for driving star-forming events on the observed
scales of many kpc along spiral arms.

Of course in these spiral systems the collision mean free path of
"phase I" clouds may be short enough to treat the ensemble of clouds as
a dissipative continuum (see Shu 1977). In this case the dynamics of
the "phase I" gas may dominate that of the "Phase III" gas and lead to
shocks and high compressions involving large increases in the number of
clouds per unit volume in spiral arms (as in Figure 1) despite the
presence of "Phase III" gas throughout.

Alternatively "Phase III" gas may not be prevalent throughout both
arm and interarm regions (Scott, Jensen, and Roberts, 1977). Indeed
"Phase III" gas is likely to be formed primarily in the supernovae-rich
spiral arms. The cooling time for this gas is shorter than the time it
takes for the gas to travel between spiral arms (Smith 1977).   Con-
sequently the "Phase III" gas may dominate the intercloud medium only
near spiral arms, where most supernovae occur. The "Phase III" gas
might then cool to a "Phase II" medium in the interarm region. This
newly-cooled medium could then experience a shock upon encountering the
next density wave enhancement, and the shock wave could produce more
young stars, some fraction of which would result in supernovae which
could in turn re-heat the interstellar medium to a "Phase III" tempera-
ture, thus completing the cycle.

REFERENCES

Bash, F. N. and Peters, W. L. 1976, Ap. J., 205, 786.
Burton, W. B. 1971, Astron. & Astrophys., 10, 76.
Burton, W. B. 1976, Ann. Rev. Astron. & Astrophys., 14, 275.
Burton, W. B. and Gordon, M. A. 1976, Ap. J. (Letters), 207, L189.
Burton, W. B. and Gordon, M. A. 1977a, Astron. & Astrophys., submitted.
Burton, W. B. and Gordon, M. A. 1977b, in "Topics in Interstellar Mat-
       ter", H. van Woerden (ed.), Reidel, Dordrecht.
Burton, W. B., Gordon, M. A., Bania, T. M., and Lockman, F. J., 1975,
       Ap. J., 202 30.

Burton, W. B. and Shane, W. W. 1970, Proc. I.A.U. Symp. No. 38, 397.
Caster, J., McCray, R., and Weaver, R., 1975, Ap. J. Lett., 200, L107.
Clark, B. G., 1965, Ap. J., 142, 1398.
Cox, D. P., and Smith, B. W., 1974, Ap. J. Lett., 189, L105.
Field, G. B., Goldsmith, D. W., and Habing, H. J., 1969, Ap. J. Lett., 155, L149.
Fujimoto, M. 1968, Proc. I.A.U. Symp. No. 29, 453.
Gordon, M. A. and Burton, W. B. 1976, Ap. J., 208, 346.
Hughes, M. P., Thompson, A. R., and Colvin, R. S., 1971, Ap. J. Suppl., 23, 323.
Huntley, J. M., Sanders, R. H., and Roberts, W. W., 1977, Ap. J., submitted.
Jenkins, E. B. and Meloy, D. A., 1974, Ap. J. Lett., 193, L121.
Kodaira, K., 1974, Publ. Astron. Soc. Japan, 26, 255.
Kraushaar, W. L., 1977, Invited Lecture at A.A.S. meeting, Honolulu.
Lin, C. C. 1971, in Highlights of Astr., 2, 88, Reidel, Dordrecht.
Lindblad, B. 1963, Stockholm Obs. Ann., 22, 3.
Lockman, F. J., 1976, Ap. J., 209, 429
Mark, J. W.-K. 1971, Proc. Natl. Acad. Sci., 68, 2095.
Mark, J. W.-K. 1974, Ap. J., 193, 539.
McKee, C. F., and Ostriker, J. P., 1977, preprint.
Oort, J. H. 1973, Proc. I.A.U. Symp. No. 58, 375.
Pikel'ner, S. B., 1967, Astron. Zh., 44, 1915.
Radhakrishnan, V., Murray, J. D., Lockhart, P., and Whittle, R. P. J., 1972, Ap. J. Suppl., 203, 15.
Roberts, M. S. 1974, Science, 183, 371.
Roberts, W. W. 1969, Ap. J., 158, 123.
Roberts, W. W. 1975, Vistas in Astron., 19, 91.
Roberts, W. W., and Burton, W. B., 1977, in "Topics in Interstellar Matter," H. van Woerden (ed.), Reidel, Dordrecht.
Roberts, W. W., Roberts, M. S., and Shu, F. H. 1975, Ap. J., 196, 381.
Roberts, W. W. and Yuan, C. 1970, Ap. J., 161, 877.
Rots, A. H. 1975, Astron. & Astrophys., 45, 43.
Rots, A. H., and Shane, W. W. 1975, Astron. & Astrophys., 45, 25.
Sanders, R. H., and Huntley, J. M., 1976, Ap. J., 209, 53.
Sawa, T. 1975, Sci. Reports Tohoku Univ. Series 1, LVIII, 13.
Scott, J. S., Jensen, E. B., and Roberts, W. W., 1977, Nature, 265, 123.
Scoville, N. Z. and Solomon, P. M. 1975, Ap. J. (Letters), 199, L105.
Segalovitz, A. 1975, Astron. & Astrophys., 40, 401.
Shu, F. H. 1973, Am. Sci., 61, 524.
Shu, F. H. 1975, Proc. Colloquium on Spiral Galaxies, Bures-sur-Yvette, 309
Shu, F. H., 1977, Proc. I.A.U. Symp. No. 77, Bad Munstereifel.
Shu, F. H., Milione, V., Gebel, W., Yuan, C., Goldsmith, D. W., and Roberts, W. W. 1972, Ap. J., 173, 557.
Shu, F. H., Milione, V., and Roberts, W. W. 1973, Ap. J., 183, 819.
Smith, B. W., 1977, preprint.
Sorensen, S. A., Matsuda, T., and Fujimoto, M., 1976, Astrophys. Space Sci., 43, 491.

W.W. Roberts, Jr.

Spitzer, L., Jr., and Jenkins, E. B., 1975, Ann. Rev. Astr. Astrophys.,
    13, 133.
Spitzer, L., Jr. and Scott, E. H., 1969, Ap. J., 157, 161.
Stecker, F. W., Puget, J. L., Strong, A. W., and Bredekamp, J. H., 1974,
    Ap. J. Lett., 188, L59.
Steigman, G., Strittmatter, P. A., and Williams, R. E., 1975, Ap. J.,
    198, 575.
Strong, A. W., 1975, J. Phys. A., 8, 617.
van den Bergh, S., 1960a, Ap. J., 131, 215.
van den Bergh, S., 1960b, Ap. J., 131, 558.
Visser, H. C. D., 1977, Proc. I.A.U. Symp. No. 77, Bad Munstereifel.
Weaver, R., McCray, R., Caster, J., Shapiro, P., and Moore, R., 1977,
    preprint.
Woodward, P. R., 1976, Ap. J., 207, 484.
Yuan, C. 1969, Ap. J., 158, 871.